Chemical Engineering Journal 108 (2005) 257–268

Chemical Engineering Journal

www.elsevier.com/locate/cej

Paired electrolysis in a solid polymer electrolyte reactor—Simultaneously reduction of nitrate and oxidation of ammonia

H. Cheng *, K. Scott, P.A. Christensen

School of Chemical Engineering & Advanced Materials, University of Newcastle upon Tyne, Newcastle upon Tyne NE1 7RU, UK

Received 8 September 2004; received in revised form 8 February 2005; accepted 11 February 2005

Abstract

Simultaneous reduction of nitrates and oxidation of ammonia in aqueous solutions have been carried out in a zero gap solid polymer electrolyte (ZGSPE) reactor, operated galvanostatically in a batch recycle mode. Complete removal of 16.1 mM nitrate and 9.4 mM ammonia was achieved within 45 h with removal rates of 0.057 mol NO_3^- cm^{-2} h^{-1} and 0.017 mol NH_3 cm^{-2} h^{-1}. Space–time yields of 5.4 kg NO_3 m^{-3} h^{-1} and 0.17 kg NH_3 m^{-3} h^{-1}, current efficiencies for nitrogen formation of 24.5% in the nitrate reduction and 1.4% in the ammonia oxidation and energy consumptions of 40.1 kWh (kg $NO_3^-)^{-1}$ were obtained during nitrate reduction, no nitrite was formed and N_2 was the main product under the best conditions. However, an improvement in the selectivity for the ammonia oxidation towards nitrogen is required. Effects of reactant concentrations, temperature and flow rate have been investigated. Use of the ZGSPE reactor could treat a wide range of wastes containing nitrate and ammonia, including those with very low levels of nitrate ions and ammonia.
© 2005 Elsevier B.V. All rights reserved.

Keywords: Paired electrolysis; Ammonia oxidation; Nitrate reduction; Zero gap solid polymer electrolyte reactor; $PdRh_{1.5}$ cathode; Pt anode

1. Introduction

Intensive use of fertilisers in agriculture and nitrate salts in some industrial sectors, e.g. the nuclear industry, causes severe nitrate pollution in many sources of water and industrial sites [1,2]. Performance assessment of low-level wastes indicates that nitrate and nitrite are among the major contributors to potential environmental release and personnel exposure [3]. Ammonia is a common and highly toxic component in gaseous and aqueous waste streams, and its destruction has therefore become a prominent topic in environmental catalysis [4]. Since nitrite can convert to carcinogenic nitrosoamines in food products and within the human digestive system [5] and ammonia can damage internal organ systems of human beings and higher animals at 1 ppm level [6,7], the allowable concentrations of these species are very low, e.g. 50 mg NO_3^- dm^{-3} (15 mg NO_3^- dm^{-3} for infants) [1,8], 0.5 mg NO_2^- dm^{-3} [1,9] and 0.5 mg NH_3 dm^{-3} [6,7]. Intensive investigation has contributed to understand the nitrate reduction reaction and to develop technologies for removal of nitrate from drinking water and wastewater [2,10].

Early treatment of nitrate wastes used calcination, which is unattractive now because it requires high temperatures and pressures, it forms sodium nitrate melts and releases toxic off-gases, e.g. NO_x [11,12]. Among current technologies used to remove nitrate from aqueous solutions, ion exchange and reverse osmosis only separate rather than destroy nitrate, produce secondary brine wastes and require frequent regeneration of the media, which introduced new pollution [10,13–15]. Biological treatment of nitrate at millimolar levels was considered as a more economic process than ion exchange, electrodialysis and chemical reduction, which can remove nitrates down to 2–10 mg l^{-1} of total nitrogen. However, biological denitrification is slow and incomplete, it requires intensive maintenance and constant supply of organic substrates and chlorine, and it causes problems of disposal of biomass sludge and contamination of denitrified water by bacteria and/or produced toxic nitrous oxide or nitric oxide [11,12,14–17]. Chemical reduction of nitrate using hydrogen or metals, e.g. iron and Pd-based catalysts, has been attractive [14,18,19], but low effectiveness, disposal

* Corresponding author. Tel.: +44 191 222 5207; fax: +44 191 222 5292.
E-mail address: hua.cheng@ncl.ac.uk (H. Cheng).

1385-8947/$ – see front matter © 2005 Elsevier B.V. All rights reserved.
doi:10.1016/j.cej.2005.02.028

of large amounts of sludge and ammonia, concerns of the process stability and safety and high costs prevented its wide application [12,20,21].

Electrochemical reduction has been proposed as an alternative technology for removal of nitrates, nitrites and ammonia through the following reactions, for example, in alkaline media [2,10,13,22–30]:

Nitrate reduction

$$NO_3^- + H_2O + 2e^- = NO_2^- + 2OH^- \quad (1)$$

$$NO_3^- + 3H_2O + 5e^- = \tfrac{1}{2}N_2 + 6OH^- \quad (2)$$

$$NO_3^- + 6H_2O + 8e^- = NH_3 + 9OH^- \quad (3a)$$

$$NO_2^- + 2H_2O + 3e^- = \tfrac{1}{2}N_2 + 4OH^- \quad (4)$$

$$NO_2^- + 5H_2O + 6e^- = NH_3 + 7OH^- \quad (5a)$$

Ammonia oxidation

$$NH_3 + 3OH^- = \tfrac{1}{2}N_2 + 3H_2O + 3e^- \quad (6)$$

$$NH_3 + 9OH^- = NO_3^- 6H_2O + 8e^- \quad (3b)$$

$$NH_3 + 7OH^- = NO_2^- 5H_2O + 6e^- \quad (5b)$$

Compared to other methods, e.g. ion exchange, electrochemical reduction was relatively simple because it used less operation steps. The disposal volume of waste in an electrochemical process could be decreased significantly, by up to 75%; due to recycle of the hydroxide produced [2,3,10,13,22–25].

Significant research has gone into the search for active, selective and efficient cathode materials for nitrate reduction [11]. Transition metals, i.e. Pt, Pd, Rh, Ru and Ir, and coinage metals, i.e. Cu, Ag and Au, have been researched, particularly in acidic media [13,31–33]. More recent attention has moved to binary and ternary catalysts, e.g. Pd–Ge, Pt–Pd, Pd–Cu and Pt–Pd–Ge [34–36]. In addition to high activity, high selectivity could be achieved through the use of bimetallic electrodes. For instance, during the reduction of nitrate with Pd/Cu electrodes, the main product was nitrogen at low Cu coverage and the amount of N_2O increased as the Cu coverage increased [36]. Very recently, a patent was applied for the electrolytic removal of nitrate containing water using an Rh coated cathode in which the nitrate ions were converted to nitrogen gas [37]. New materials, e.g. B-doped diamond [38,39], Dawson-type heteropolyanions, $P_2W_{12}Mo_5Cu$ or $P_2W_{15}Mo_5Ni$ [40,41], phthalocyanine complexes of Mn, Fe, Co, Ni, Cu and Zn [42] and hydrogen storage alloys, e.g. M $(NiAlMnCo)_5$ (M = La, Ce and Pr) [43], have been used in the electrochemical reduction of nitrate with ammonia as the main product. However, the suitability of these materials for a technical process has not yet been tested. Use of engineering materials such as packed particle bed electrodes (Cu, Ni, Fe or Pb) has led to a significant decrease in the concentration of the nitrate, e.g. from 1000 to 50 mg dm^{-3} with a current efficiency of 40%, in low-level nuclear waste due to high interfacial surface area and enhanced mass transfer [10]. A new technique combining electroreduction and electrocoagulation was used to remove nitrate from water, which led to a decrease of nitrate concentration from 100 to 30 mg dm^{-3}, with a very low energy consumption of 0.05 kWh kg^{-1} [44].

Reduction of both nitrate and nitrite in acidic media occurs at more positive potentials than in alkaline media [13,45–48] and nitrate reduction occurs on Cu, Cd and Zn, but not on Ni and Pb in acid solutions [49]. Product distribution was highly dependent on the pH of the solution, e.g. ammonia was produced favourably at low pH [50,51], and on potential, i.e. ammonia formed under most potentials but a reduction to nitrogen only occurred at certain potentials [52]. Both ammonia and hydroxylamine were reported as major products in strong acid (>5 M H^+) [53].

Reduction of nitrate in alkaline media has attracted a lot of fundamental and applied research in several industrial sectors [2]. For example, in concentrated NaOH solutions, the nitrate concentration decreased from 600 to 50 mg dm^{-3} with a current efficiency of 22% using a flow-through reactor with a Cu electrode [17]. A reduction of the nitrate concentration from 1000 to 18 mg dm^{-3} was achieved in weakly alkaline solution, i.e. a $NaHCO_3$ solution [10].

At the moment, the industrial use of electrochemical nitrate removal is challenged in several ways, e.g. low selectivity to nitrogen, formation of nitrite intermediate and release of ammonia [12,13], unsuitable electrodes [21,25,54], deposition of metal impurities on the cathode and changing cathode properties [55], release of off-gases, requirements of significant quantities of make-up water and disposal of NaOH by-product [13].

The electrochemical oxidation of ammonia in aqueous alkaline solutions at high surface area platinum electrodes has been the subject of several studies because of drawbacks of other technologies, e.g. high cost with low effectiveness in bacterial degradation [56]. The oxidation mechanism was a major topic of early work [57–60]. The research attracted industrial interest, especially for removal of ammonia from wastewater [61]. A typical example is oxidising ammonia in an undivided flow cell with platinised graphite, Ti or Ta anode and stainless steel cathode during secondary sewage treatment. The NH_3 was oxidised to nitrogen with 25–57% of removal and current efficiencies between 13.5 and 28.2% for treatment of a typical sewage effluent, i.e. 30 mg dm^{-3} ammonia at pH 8. The main barrier for scale-up was high capital investment [61].

Platinum was considered as the best anode material for ammonia oxidation because it was able to prevent formation of poisoning species, e.g. N_{ads}, and to stabilise active species, e.g. NH_{ads}. The former could block the electrode surface and the latter could combine to N_2H_x (x = 2–4) adspecies and then to form N_2. Lower activity and selectivity was observed on ruthenium, rhodium, palladium and iridium electrodes. Gold, silver and copper only showed low activity [57,62–66].

One of the major problems in the electrochemical reduction of nitrate is production of ammonia, which caused

environmental concern and was unallowable in some industrial sectors, e.g. drinking water industry [42,54]. Therefore, it was our aim to establish a technical process based on paired electrolysis, i.e. perform nitrate reduction and ammonia oxidation simultaneously, in a zero gap solid polymer electrolyte (ZGSPE) reactor to remove both nitrate and ammonia. The reactor was evaluated in terms of percentages and rates of nitrate and ammonia removal, selectivity, current efficiency and energy consumption. To our best knowledge, this is a first report using a zero gap solid polymer electrolyte reactor for simultaneous reduction of nitrate and oxidation of ammonia.

2. Experimental

2.1. Materials and chemicals

The following materials and chemicals were used as received: Ti mini-mesh (Ti purity 99.6%, mesh size 1.5 mm, open area 37%, wire diameter 0.2 mm, Goodfellow), $PdCl_2$ (99%, Aldrich), $RhCl_3$ (98%, Aldrich), $NaNO_3$ (99.99%, Aldrich), $NaNO_2$ (99.99%, Aldrich), $NaHCO_3$ (99.7%, Aldrich), NH_4Cl (99.5%, Aldrich), NaOH (99.99%, Aldrich), NaCl (99%, Aldrich), Na_2SO_4 (99%, Aldrich), H_2SO_4 (98%, AnalaR, BDH), NH_3 (35% aqueous solution, AnalaR, BDH) and phthalic acid (99.5%, Aldrich).

A model simulating spent solution after strongly basic anion exchanger regeneration in the drinking water treatment industry was used as catholyte in this study. The solution consisted of 84.0 g dm^{-3} (1 M) $NaHCO_3$, 0.4 g dm^{-3} (6.8 mM) NaCl, 0.4 g dm^{-3} (2.8 mM) Na_2SO_4 and 1.0 g dm^{-3} (1000 ppm, 16.1 mM) NO_3^- (in the form of $NaNO_3$) [10]. The nitrate concentration was changed in several experiments. Anolytes used were the catholytes obtained from the nitrate reduction or simulated those discharged from the sewage, which contained low concentrations of ammonia [61]. Fresh electrolytes were used for each paired electrolysis.

All solutions were prepared using deionised water obtained from an ELGASTAT B124 Water Purification Unit (The Elga Group, England).

2.2. Electrode

Pd–Rh titanium mini-mesh electrodes were thermally deposited. The mesh was made of woven titanium wires having mesh apertures of 2 mm and had a very open structure for delivering reactants and products. It was first abraded with emery paper and rinsed thoroughly with water and rinsed in acetone. Following etching with boiling 37% HCl solution for 5 min, the mesh was put into an oven set at 500 °C for 10 min. After cooling and weighing, the mesh was dipped in ethanol solutions containing the metal salts (0.2 M) and then put into the oven at the deposition temperature (500 °C), in air, for 10 min. The dip-heating procedure was repeated until the desired catalyst loading was achieved. The binary catalysts were obtained by depositing the first component followed by depositing the second constitute and repeating the procedure. The deposited mesh was annealed at the deposition temperature (500 °C) for 3 h then allowed it cool naturally to ambient temperature. The catalyst loading was obtained by weight difference of the mesh before and after deposition assuming those most stable oxides were formed during the deposition, i.e. PdO and Rh_2O_3 [26]. Finally, the deposited mesh was post-treated by electrolysis in an undivided cell using the deposited mesh as cathode and a Pt mesh as anode in 0.25 M H_2SO_4 aqueous solution at a constant current density of 2 mA cm^{-2} for 30–60 min. At the start, the electrolyte became dark in colour, possibly due to dissolution of the catalysts; the solution was clear again at the end of the electrolysis, possibly, the dissolved catalysts were deposited onto the mesh again. The prepared binary electrode was assigned as $PdRh_{1.5}$ according to the atomic ratio of the two metals.

2.3. Solid polymer electrolyte reactor

A zero gap (i.e. electrodes and SPE are in direct contact) solid polymer electrolyte reactor was used to treat the nitrate solutions under various conditions (Fig. 1). The reactor

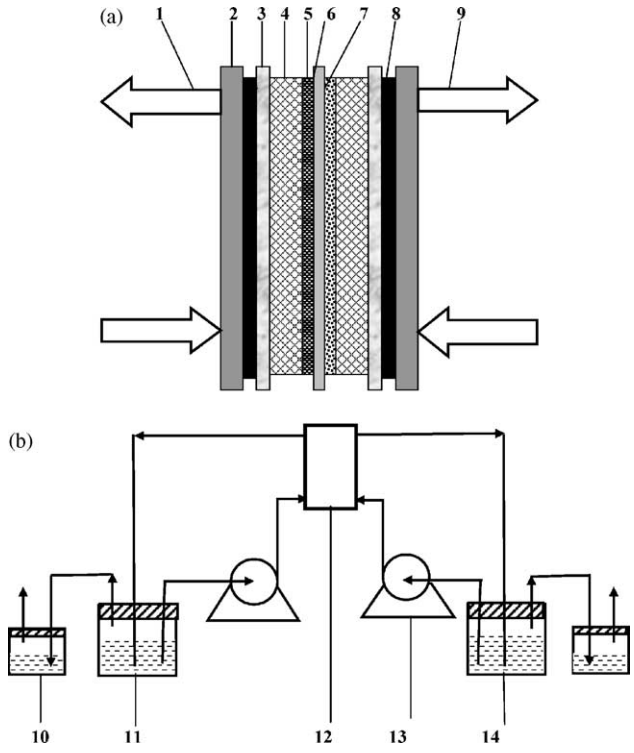

Fig. 1. (a) Zero gap solid polymer electrolyte reactor—1: catholyte; 2: end plate (stainless steel); 3: manifold plate (PTFE); 4: distributor (stainless steel mesh); 5: cathode ($PdRh_{1.5}$/Ti mini-mesh); 6: Nafion® 117 membrane; 7: anode (Pt/Ti mini-mesh); 8: seal O-ring (Tiron rubber); 9: anolyte. The cell dimension is 22 cm × 14 cm × 3 cm. (b) Flow diagram—10: gas adsorbent reservoir; 11: catholyte reservoir; 12: zero gap solid polymer electrolyte reactor; 13: pump; 14: anolyte reservoir.

consisted of a membrane–electrode assembly (MEA), two stainless steel back-plates (15 cm × 10 cm × 2 cm each), two PTFE channelled plates (15 cm × 10 cm × 2 cm each) with six channels (2 mm in width, 1 mm in depth and 25 mm in length), eight layers of stainless steel mesh (current collectors and turbulence promoters) and two Tiron rubber O-ring [67]. The main part of the reactor was a sandwiched membrane electrode assembly (MEA, 0.6 mm in thickness and 20 cm^2 in active area) obtained by hot pressing the mesh anode and the mesh cathode on either side of the pre-treated Nafion® 117 membranes at 50 kg cm^{-2} and 100 °C for 3 min [68]. A Nafion® 117 membrane was used to retain the nitrate ions in the cathode chamber and thus to obtain reliable data for the concentration change of nitrate ions. In the reactor, the cation Na^+, rather than H^+, acted as the charge carrier in the solid electrolyte.

The reactor was inserted into a circulation loop consisting of anolyte and catholyte peristaltic pumps (Cole-Parmer) and reservoirs (1 dm^3) placed in two heating mantles (Electrothermal® Flask/Funnel, Cole-Parmer). After conditioning the MEA at 60 °C and atmospheric pressure with continuous feed of 0.5 M H_2SO_4 solution for 24 h, the reactor was used under various operating conditions in a batch recirculation mode. The off-gases were introduced into reservoirs containing 1 M H_2SO_4 aqueous solutions before venting to the atmosphere. The reactor rig was operated in a closed loop so no separation and recycling of a supporting electrolyte, which exists in waste, was required.

2.4. Electrochemical measurements

The polarisation curves were measured in a three-electrode, two-compartment cell divided by a Nafion® 117 membrane using cyclic voltammetry and steady-state polarisation measurements. A potentiostat set, which consisted of a Ministat Potentiostat, a PCI-100 computer interface and an EC Prog v3 Software (Sycopel Scientific Limited) was used for all voltammetric and steady-state measurements. The working electrodes were a $PdRh_{1.5}$/Ti mini-mesh (0.75 mg Pd + 1.09 mg Rh cm^{-2}, 1.2 cm^2) for nitrate reduction and a Pt/Ti mini-mesh (2.03 mg Pt cm^{-2}, 1.2 cm^2) for ammonia oxidation. A commercial saturated calomel electrode (SCE, Russel) and a platinum mesh (20 cm^2) were used as reference and counter electrodes, respectively. All potentials are quoted against the SCE reference electrode. All of the solutions studied were thoroughly degassed using oxygen free nitrogen (BOC Ltd.). The $PdRh_{1.5}$ or the Pt working electrodes were cycled three times between 0.4 and −1.2 V or 0.4 and 1.6 V at a scan rate of 50 mV s^{-1} before collecting stable polarisation data.

2.5. Batch electrolysis

Batch electrolysis was performed in the ZGSPE reactor controlled at a constant current density (1, 5, 10 or 20 mA cm^{-2}) using a FARNELL LS60-5 power supply for periods up to 150 h. The electrolytes were flowed at a constant rate, i.e. 15, 50 or 100 cm^3 min^{-1}. Samples were taken at regular intervals and were analysed for concentrations of NO_3^-, NO_2^-, NH_3 and pH, etc. One molar H_2SO_4 solutions (50 ml for each chamber) were used as absorbent for the released ammonia [43], if any. The final data included ammonia detected in the absorption solution.

2.6. Product analysis

High-performance liquid chromatography (HPLC) was performed in a DIONEX HPLC system, which consisted of a P 580 Pump and a Softron 2000 UVD 170S/340S UV/Vis detector with a Whatman Partisil 5 ODS-3 column (5 μm particle size and 25 cm × 0.46 cm, Alltech Associates, Inc.). The wavelengths used in HPLC measurements were determined using UV–vis spectroscopy (UV-160A UV–Visible Recording Spectrophotometer, SHIMADZU, Japan). Normally, the UV detector was set to 320 nm for nitrate detection and 360 nm for nitrite detection. The mobile phase was a 4 mM phthalic acid aqueous solution with a flow rate of 1.0 cm^3 min^{-1}. The peaks for nitrate ions (retention time, 3.15 min) and nitrite ions (retention time, 3.90 min) were characterised by using standard solutions. Quantification of the product distribution during the electrolysis was accomplished by use of calibration curves with the authentic samples (Aldrich). The calibrations for the standard solutions (1.0×10^{-5} to 0.2 mol dm^{-3}) were carried out three times for each compound and the data were averaged. A sample volume of 20 μl was generally employed. The detection limits of this method were 1 ppm for nitrate ions and 0.3 ppm for nitrite ions under the experimental conditions.

Ammonia was analysed with an Orion Model 95-12 Ammonia (NH_3) Gas Sensing Combination Electrode connected to an Orion digital Ion/pH meter (Corning Model 135, Corning Glass Works or Orion model 920A, Orion Research, Inc.). Calibration curves were obtained using standard solutions of 5×10^{-5} to 0.15 mol dm^{-3} NH_4Cl, prepared using the standard ammonium chloride solution (Orion 951006) and the ionic strength adjustor solution (Orion 951211) at the operational temperature. The calibrations were carried out before and after each experiment. The sample for determining ammonia was prepared by putting 1–5 cm^3 samples into a 25 cm^3 standard flask and adding an ionic strength adjustor solution (Orion 951211) to the mark of the flask before the measurement was carried out. A 50 ml 1 M H_2SO_4 solution acted as absorbent for the produced ammonia [43], if any. The detected ammonia concentration of the collective solution was included in the product distribution.

A reported method was used to obtain the amount of nitrogenous gas formed, which was deduced from the total nitrogen concentration in solution measured before and after the electrolysis [6,21]. No evidence for other probable liquid products, such as hydroxylamine (NH_2OH) and hydrazine (N_2H_4), was found in our electrolysed solutions using the

standard chemical analysis methods [69], which is similar as reported previously [60].

2.7. Parameter definitions

Reactor performance was evaluated based on activity using normalised percentage of nitrate or ammonia removal (χ), space–time yield (γ) and average rate of nitrate or ammonia removal (β); selectivity using yields of nitrogen (ξ_{N_2}), ammonia (ξ_{NH_3}), nitrite (ξ_{NO_2}) and nitrate (ξ_{NO_3}) and efficiency using current efficiency (ϕ_i or ϕ) and energy consumption (ψ_i or ψ_R). The parameters are defined as [70–73]:

$$\chi = \frac{C_0 - C_t}{C_0} \times 100\% \quad (7)$$

$$\gamma_i = \frac{3600 \times \alpha \times j \times \phi_i \times M_{FW}}{n_i \times F} \quad (8a)$$

$$\gamma = \sum \left(\frac{C_i}{C_0 - C_t} \times \gamma_i \right) \quad (8b)$$

$$\beta = \frac{(C_0 - C_t) \times V}{t \times A} \quad (9)$$

$$\xi_i = \frac{C_i}{C_0 - C_t} \times 100\% \quad (10)$$

$$\phi_i = \frac{m_i \times n_i \times F}{q} \quad (11a)$$

$$\phi = \sum \phi_i \quad (11b)$$

$$\psi_i = \frac{n_i \times F \times E_{cell}}{\phi_i \times M_{FW}} \quad (12a)$$

$$\psi_R = \sum \left(\frac{C_i}{C_0 - C_t} \times \psi_i \right) \quad (12b)$$

where C_0 and C_t are concentrations of nitrate or ammonia (mol dm^{-3}) at the start and at the electrolysis time t (h), respectively, C_i the concentration of nitrogen, ammonia, nitrite or nitrate (mol dm^{-3}) at t (h), α the specific area (m^{-1}), defined as a ratio of the electrode area to the volume of the batch of solution undergoing treatment, j the current density (A m^{-2}), n_i is the number of electrons in the reaction forming i (i = nitrogen, ammonia, nitrite, nitrate, etc.), F the Faraday constant (96,485 C mol^{-1}), M_{FW} the molar mass of nitrate ions or ammonia (kg mol^{-1}), V the volume of the batch of solution undergoing treatment (dm^3), A the geometric area of cathode (m^2), m_i the quantity of the formed species i (mol), q the total electrical charge (C) and E_{cell} is the cell voltage. ψ_i, and ψ_R are energies consumed for formation of i, nitrate reduction and ammonia oxidation, respectively.

Considering the fact that different percentages of initial reactants, i.e. $NaNO_3$ or NH_3, were converted to intermediates according to Eqs. (1), (2), (3a), (3b) in alkaline solutions, a weighting parameter (equal to $\frac{C_i}{C_0 - C_i}$) was introduced in Eqs. (8b) and (12b) to calculate the contribution to the total value of a parameter from each reaction.

Most parameters were normalised to catalyst loading unless otherwise stated.

3. Results and discussion

3.1. Voltammetric characteristics

Fig. 2 shows a cyclic voltammogram using normalised current density obtained on a $PdRh_{1.5}$/Ti mini-mesh electrode in the simulating solution with or without 0.1 M $NaNO_3$ [10] at ambient temperature. The figure shows a cathodic plateau between −0.70 and −0.80 V versus SCE in the blank solution due to reduction of species in solution. The current increased rapidly after −0.80 V, which was attributed to hydrogen evolution in the medium, as evidenced by the fact that gas bubbles were evolved violently from the electrode surface. A broad anodic peak was observed at −0.41 V due to oxidation of the unspecified electroactive species from the hydrogen evolution. The addition of 0.1 M NO_3 led to an increase in reduction currents below potentials of −0.48 V, thus indicating the formation of an active surface on the electrode for the reduction of nitrate, in addition to the species leading to the hydrogen evolution. The figure clearly shows that, in the presence of NO_3, the significant change of the oxidation peak, i.e. decrease in the peak current density and a negative shift of the peak potential from −0.41 to −0.69 V, was accompanied by an increase in the reduction current due to nitrate reduction (Fig. 1). These shifts imply a change of the electrode surface due to nitrate reduction [42], possibly, the intermediates and/or products of nitrate ions at the $PdRh_{1.5}$/Ti

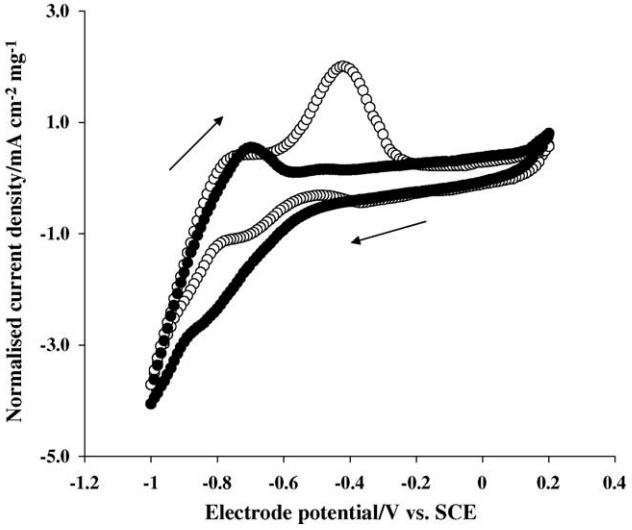

Fig. 2. Cyclic voltammetric curves on the $PdRh_{1.5}$ mini-mesh electrode in the alkaline solution with and without nitrate ions. Cell: H-cell divided by a Nafion® 117 membrane. Cathode: $PdRh_{1.5}$ (0.75 mg Pd + 1.09 mg Rh cm^{-2}, 1.3 cm^2). Anode: Pt mesh (20 cm^2). Catholyte: the simulated solution with (●) or without (○) 0.1 M $NaNO_3$ (100 cm^3). Anolyte: 1.0 M $NaHCO_3$ solution (100 cm^3). Scan rate: 5 mV s^{-1}. Temperature: 17.5 ± 1.0 °C. The arrows indicate scan directions.

mini-mesh electrode caused inhibition of the oxidation reaction, compared to the blank solution, which has been previously reported [13]. Overall, the results of voltammetric measurements demonstrated strong involvement of hydrogen species, which were reduced simultaneously in the potential region of nitrate reduction and that the generated hydrogen adatoms on the electrode surface took part in nitrate reduction [43]. The presence of adsorbed nitrate ions and hydrogen species at the cathode surface during the nitrate reduction has been confirmed [21,74,75]. The hydrogen adatoms competed with nitrogen species for the active sites and thus hindered nitrate reduction or, successively, the released hydrogen atoms hydrogenated the intermediates formed [2,5–7]. The effect became important in the potential region of intense hydrogen evolution.

The effectiveness of the $PdRh_{1.5}$/Ti mini-mesh electrode for nitrate reduction can be attributed to the intrinsic activity of the Rh and Pd for nitrate reduction and, more importantly, to the synergetic effects, which resulted from the local electronic modification or the co-operative electronic effects as well as active sites distribution induced by mixing different catalysts [76–78]. The metal–metal combination modified the electronic environment and changed the structure parameters, such as bonding distance and bonding energy, reaction mechanism, etc., compared to single catalysts. Such an effect has been demonstrated for nitrate reduction and the binary and ternary catalysts showed better catalytic activity than the single catalysts in terms of the reduction of nitrates and preventing formation of ammonium [18,19].

Steady-state polarisation curves obtained on a Pt/Ti mini-mesh working electrode in the 1 M NaOH solution with (0.1 M) or without ammonia are shown in Fig. 3. The current

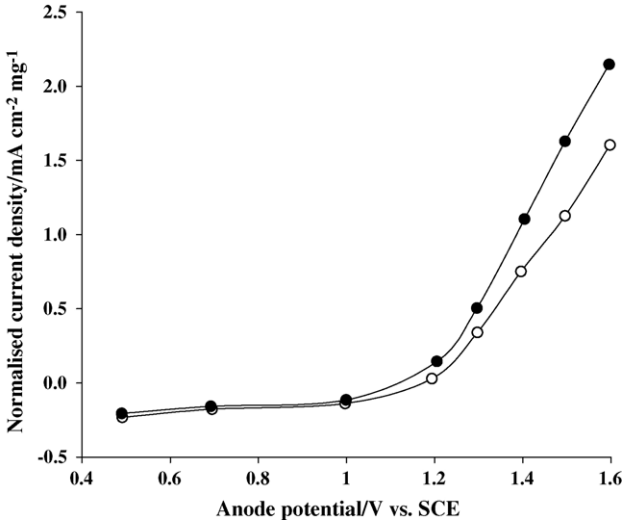

Fig. 3. Steady-state polarisation curves on the Pt/Ti mini-mesh electrode in 1 M NaOH solution with and without ammonia. Anode: Pt/Ti mini-mesh (2.03 mg Pt cm^{-2}, 1.2 cm^2); Cathode: Pt mesh (20 cm^2). Anolyte: 1.0 M NaOH solution with (●) or without (○) 0.1 M NH_3 (100 cm^3). Catholyte: 1.0 M NaOH solution (100 cm^3). The data were collected using potentiostatic measurements and other conditions as in Fig. 2.

increased after the rest potential, i.e. 1.19 V versus SCE, as compared to that observed in the blank solution, suggesting that ammonia was oxidised on the Pt/Ti mini-mesh electrode. The data were in agreement with those reported using platinised Pt electrode under similar conditions [60,79]. The activity of the Pt anode for the ammonia oxidation resulted from its intrinsic property and the interaction between the polarised electrode and ammonia. It was believed that the anodic polarisation of the Pt electrode surface during ammonia oxidation led to an excess positive charge and thus lowered the Fermi level of the Pt metal and resulted in a decrease of the electron density in the ammonia orbitals. Consequently, the Pt–N bonds were strengthened and the N–H bonds were weakened, making them more prone to dissociation [63]. Such an electronic effect prevented formation of poisoning species, e.g. N_{ads}, and stabilised active species, e.g. NH_{ads}. The former could block the electrode surface and the later could combine to N_2H_x ($x = 2$–4) adspecies and then to form N_2, as aforementioned [57,62–66].

The above results demonstrated the effectiveness of the $PdRh_{1.5}$ cathode for nitrate reduction and the Pt anode for ammonia oxidation. However, information on selectivity and efficiency were unavailable from the voltammetric measurements, although they are important criteria because nitrite ions and ammonia are more toxic than nitrate ions and their formation should be avoided. To verify the results obtained using voltammetric measurements and to determine selectivity and efficiency of the ZGSPE reactor for nitrate reduction and ammonia oxidation, batch electrolyses were carried out. The concentrations of nitrate, nitrite, ammonia and other possible side products were monitored using HPLC and ion sensor. Yields of these components were calculated according to Eqs. (1), (2), (3a), (3b), (5a) and (5b).

3.2. Bulk electrolysis—feasibility

Feasibility of simultaneous reduction of nitrate and oxidation of ammonia was demonstrated in the zero gap solid polymer electrolyte reactor using Ti mini-mesh electrodes with $PdRh_{1.5}$ or Pt catalysts. Typical data are presented in Fig. 4 where the simulated solution was used as the catholyte and a solution produced in the previous reduction of nitrate, i.e. 9.42 mM NH_4^+ in the simulated solution without NO_3^-, was used as the anolyte. Conversions of nitrate (for the nitrate reduction) and ammonia (for the ammonia oxidation) steadily increased and finally, after 50 h electrolysis, reached 100% with concomitant formation of nitrogen and ammonia or nitrate (Fig. 4; Tables 1 and 2). The concentration of nitrogen approached high values within 20 or 10 h for the nitrate reduction and the ammonia oxidation, respectively, after which the nitrogen concentrations seemed to level off. The initial increase in concentrations of nitrogen and ammonia or nitrate can be explained based on the relatively high reaction rates of Eqs. (2) and (3a) (nitrate to nitrogen and to ammonia) or (6) and (3b) (ammonia to nitrogen and nitrate). The levelling off in nitrogen concentration was

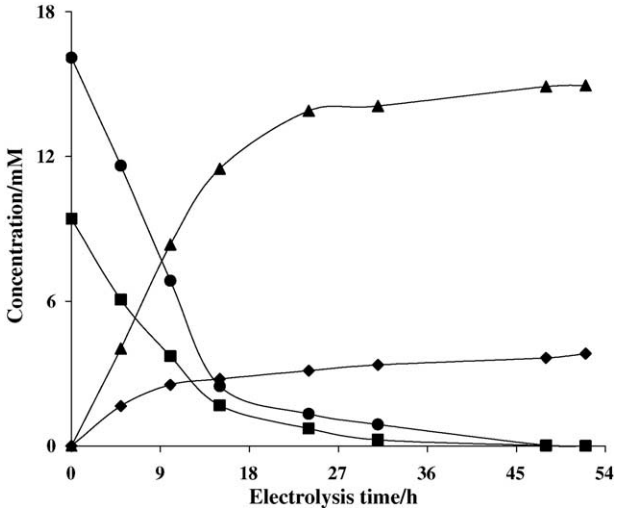

Fig. 4. Removal of nitrate and ammonia simultaneously during the paired electrolysis in a zero gap solid polymer electrolyte reactor. (●) Nitrate during the nitrate reduction; (▲) nitrogen during nitrate reduction; (■) ammonia during ammonia oxidation; (♦) nitrogen during the ammonia oxidation. Reactor: zero gap solid polymer electrolyte reactor divided by a Nafion® 117 membrane. Cathode: $PdRh_{1.5}$/Ti mini-mesh (0.75 mg Pd + 1.09 mg Rh cm^{-2}, 20 cm^2). Anode: Pt/Ti mini-mesh (2.03 mg Pt cm^{-2}, 20 cm^2). Catholyte: the simulated solution (170 cm^3). Anolyte: 9.42 mM NH_4^+ in the simulated solution without nitrate ions (170 cm). Flow rate of electrolytes: 50 ml min^{-1}. Temperature: 21.5 ± 1.0 °C.

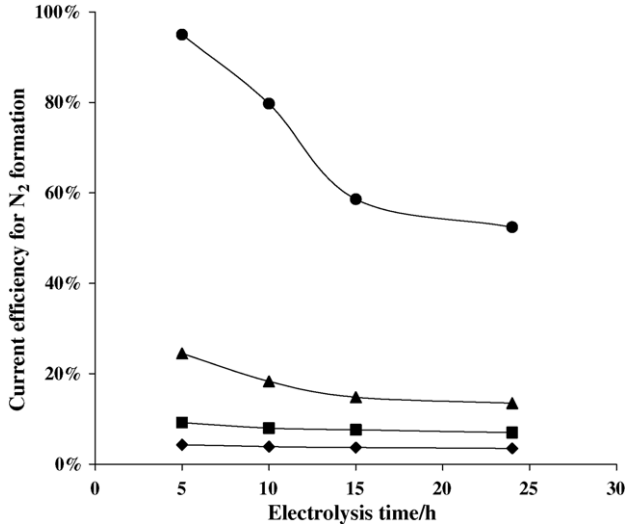

Fig. 5. Effect of controlled current density on current efficiency for nitrogen formation during the electrochemical reduction of nitrate in a zero gap solid polymer electrolyte reactor. Current density: (●) 1 mA cm^{-2}; (▲) 5 mA cm^{-2}; (■) 10 mA cm^{-2}; (♦) 20 mA cm^{-2}. Anolyte: 1.0 M $NaHCO_3$ solution (170 cm^3). Other conditions as in Fig. 4.

attributed to the decrease in concentration of reactants, i.e. nitrate or ammonia, and the consequent gradual decrease in nitrogen production rates. No nitrite ions were detected during the paired electrolysis. Other possible intermediates, e.g. NH_2OH, were also not detected, possibly, because their reduction in alkaline solutions was faster than in acidic solutions [80,81]. Thus, only overall reactions providing stable products were considered here. Investigation of other possible intermediate steps was not carried out in this work.

3.3. Bulk electrolysis—influence of current density

A significant effect of applied current density on current efficiency for both nitrate reduction and ammonia oxidation was observed. Figs. 5 and 6 show the correlation between the current density and the current efficiency for nitrogen formation in the ZGSPE reactor during the paired electrolysis. For nitrate reduction, a current density of 1 mA cm^{-2} gave the highest current efficiency, with respect to nitrate reduction to nitrogen, which was between 52.4 and 95.0% (Fig. 5). It follows from Fig. 5 that the current efficiency decreased with increasing current density. A current density of 5 mA cm^{-2}, led to lower current efficiencies, i.e. 10.8–22.5%. At higher

Table 1
Effect of current density on capacity and rate during the paired electrolysis in a zero gap solid polymer electrolyte reactor[a]

Current density (mA cm^{-2})	Catholyte			Anolyte		
	χ (%)	γ (kg m^{-3} h^{-1})	β (mol cm^{-2} h^{-1})	χ (%)	γ (kg m^{-3} h^{-1})	β (mol cm^{-2} h^{-1})
1	57.7	3.2	0.033	48.6	0.016	0.13
5	73.9	4.0	0.042	55.7	0.030	0.15
10	94.9	5.2	0.054	63.4	0.036	0.17
20	100	5.4	0.057	100	0.056	0.27

[a] The conditions as in Figs. 5 and 6.

Table 2
Effect of current density on selectivity during the paired electrolysis in a zero gap solid polymer electrolyte reactor[a]

Current density (mA cm^{-2})	Catholyte			Anolyte		
	ξ_{N_2} (%)	ξ_{NO_2} (%)	ξ_{NH_3} (%)	ξ_{NO_2} (%)	ξ_{NO_3} (%)	ξ_{N_2} (%)
1	98.9	0	1.1	0	14.1	85.9
5	97.6	0	2.4	0	42.0	58.0
10	97.1	0	2.9	0	51.9	48.1
20	92.5	0	7.5	0	65.6	34.4

[a] The conditions as in Figs. 5 and 6.

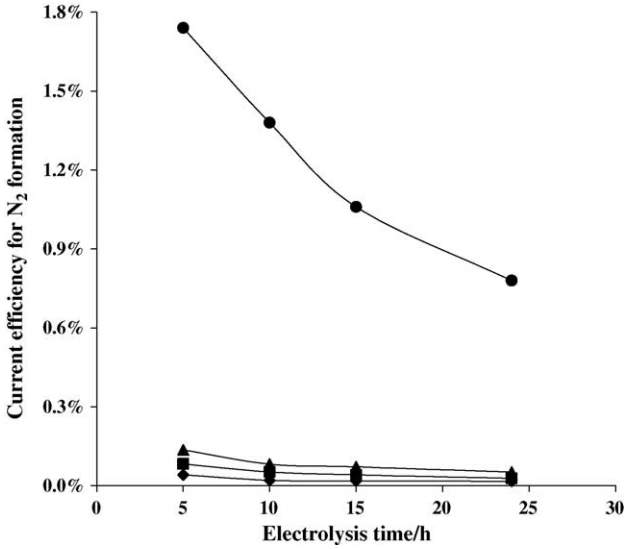

Fig. 6. Effect of controlled current density on current efficiency for nitrogen formation during the paired electrolysis in a zero gap solid polymer electrolyte reactor—ammonia oxidation. Current density: (●) 1 mA cm^{-2}; (▲) 5 mA cm^{-2}; (■) 10 mA cm^{-2}; (♦) 20 mA cm^{-2}. Catholyte: 1.0 M $NaHCO_3$ solution (170 cm^3). Other conditions as in Fig. 4.

current densities, the current efficiency decreased further, e.g. 7.0–9.2% at 10 mA cm^{-2} and 3.5–4.3% at 20 mA cm^{-2}. The decrease was probably due to higher hydrogen gas generation in the structure of the electrode restricting the access of liquid and thus limiting mass transport of nitrate to the surface of the catalyst. The data suggest that the partial current for N_2 formation at all applied current densities was between 1 and 0.5 mA cm^{-2}. A current density of 5 mA cm^{-2} was used in further study of the nitrate reduction. This was because it still exhibited a relatively high current efficiency, together with the highest partial current density for nitrate reduction to nitrogen, i.e. $\varphi \times j \approx$ constant ≈ 0.7, which was higher than that at 1 mA cm^{-2}, i.e. 0.5.

Similar trend was observed for the oxidation of ammonia on the Pt electrode, i.e. the highest current efficiencies (between 0.7 and 1.8%) were observed at a current density of 1 mA cm^{-2}, which were 40 times higher than those observed at 20 mA cm^{-2} (Fig. 6).

More data with respect to the effect of current density on the nitrate reduction and the ammonia oxidation are shown in Tables 1 and 2. Generally, increasing current density led to increases in percentage of nitrate or ammonia removal, space–time yield and average reaction rate. However, the effect was more significant from 1 to 5 mA cm^{-2} and only small change could be observed at higher current densities. For nitrate reduction, the other products changed with applied current density, e.g. ammonia yield increased from 1.1 to 7.5% when the current density increased from 1 to 5 mA cm^{-2}, i.e. the formation of ammonia was more favourable at higher current densities. It is also interesting to note the variation of solution pH with current density. The pH of the treated solutions gradually increased (more alkaline) while the anolyte became more acidic during electrolysis. The maximum pH after 24 h electrolysis was observed at 10 mA cm^{-2}, i.e. 11.59. The decrease in pH at 20 mA cm^{-2} was caused by more protons crossing the Nafion membrane. More alkaline media were beneficial to decrease nitrite and ammonia formation and to suppress hydrogen evolution during nitrate reduction [6,54]. This is one of reasons for higher current efficiencies with respect to nitrogen formation at lower current densities.

During electrolysis, hydrogen evolution took place in the potential region of nitrate reduction. So nitrate was reduced on the electrode while the generated hydrogen adatoms on the electrode surface took part in nitrate reduction. The hydrogen adatoms competed with nitrogen species for the active sites and thus hindered nitrate reduction or, successively, the released hydrogen atoms hydrogenated the intermediates formed as well as the absorbed hydrogen atom reacted with nitrate [2,5–7,21,43]. These processes determined the activity, selectivity and efficiency of the process and are important in the potential region of intensive hydrogen evolution.

The applied current density had a great effect on the product distribution during ammonia oxidation (Table 2). A decrease in the yield of nitrogen and an increase in the yield of nitrate of more than 50% were observed when the applied current density was increased from 1 to 20 mA cm^{-2}. No nitrite and hydroxylamine were detected during the oxidation, suggesting that these species, if any, were oxidised further. Similar observations were reported elsewhere [79].

It was believed that, at relatively low potentials (corresponding to relatively low current densities), the Pt was devoid of adsorbed oxygen, which benefited formation of the hydrogenated adsorbates like NH_{ads} and $NH_{2,ads}$ and led to formation of nitrogen gas. At higher potentials, adsorbed oxygen species were present at the Pt electrode surface, which promoted formation of fully dehydrogenated adsorbate, e.g. atomic nitrogen N_{ads}, which increased with time, blocked the electrode surface and thus decreased the available area for NH_3 to adsorb and dehydrogenate to active intermediates such as NH_{ads} and $NH_{2,ads}$ [62,63,79]. Consequently, lower activity and lower current efficiency were observed at higher current densities. The enhanced oxygen evolution at high current densities was also responsible for the decreased activity and selectivity with increasing current density.

3.4. Bulk electrolysis—influence of nitrate concentration, temperature and flow rate

Fig. 7 shows the results of nitrate reduction in the ZGSPE reactor using a $PdRh_{1.5}$/Ti mini-mesh cathode at a current density of 5 mA cm^{-2} in the simulated solution with different concentrations of nitrate. The data show that the rate of nitrate removal depends on nitrate concentration. When the concentration of $NaNO_3$ was smaller than 1 mM, the rate of nitrate removal was low, i.e. between 0.00027 and 0.0037 mol cm^{-2} h^{-1}. With the increase of concentration

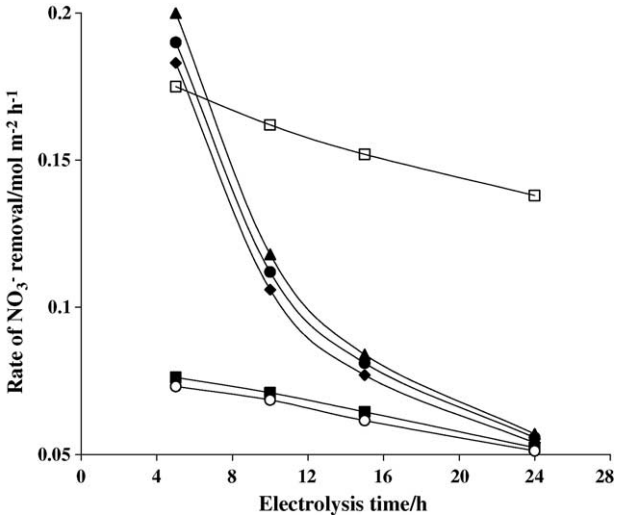

Fig. 7. Effect of nitrate concentration and temperature on rate of nitrate removal during the paired electrolysis in a zero gap solid polymer electrolyte reactor. Temperature and concentration of nitrate (the catholytes were in the simulated solution, 170 cm^3): (■) 22 ± 1.2 °C, 16.1 mM; (□) 22.5 ± 1.5 °C, 100 mM; (◯) 22 ± 1.2 °C, 16.1 mM, 100 cm^3 min^{-1}; (♦) 40 °C, 16.1 mM; (●) 60 °C, 16.1 mM; (▲) 80 °C, 16.1 mM. Other conditions as in Fig. 4.

of $NaNO_3$, the rate increased significantly, i.e. around 0.06 and 0.10 mol cm^{-2} h^{-1} in 16.1 and 100 mM solutions, respectively. A high concentration increased the mass transfer of nitrate to the electrode and thus increased the rate of nitrate removal.

Another striking feature for nitrate reduction, as shown in Table 3, is that nitrate concentration had a significant effect on space–time yield, i.e. at 24 h, 0.03, 0.3, 4.7 and 9.8 kg m^{-3} h^{-1} in 0.1, 1.0, 16.1 and 100 mM nitrate solutions, respectively. These changes were caused mainly by change in the rate of nitrate removal.

Nitrate concentration also had a great effect on the current efficiency, e.g. at 24 h, 0.09, 0.87, 13.0 and 29.2% for the nitrogen formation in 0.1, 1.0, 16.1 and 100 mM nitrate solutions, respectively (Table 3). Current efficiency was related to

Table 3
Effect of concentration of nitrate and temperature on the paired electrolysis—nitrate reduction[a]

	Concentration (mM)				
	0.1	1.0	16.1	16.1 (80 °C)	100
χ (%)	100	100	91.7	100	35.7
γ (kg m^{-3} h^{-1})	0.03	0.3	4.7	5.2	9.8
β (mol cm^{-2} h^{-1})	0.00027	0.0035	0.052	0.057	0.105
ξ_{NO_2} (%)	0	0	0	0	0
ξ_{NH_3} (%)	5.6	6.3	6.8	16.0	7.5
ξ_{N_2} (%)	94.4	93.7	93.2	84.0	92.5
ϕ (%)[b]	0.09	0.87	13.0	12.6	29.2
ψ (kWh kg^{-1})	4637.4	927.0	34.5	21.0	37.1
E_{cell} (V)	2.3	2.3	2.1	1.1	2.0

[a] Data were collected at 24 h and ambient temperature (21.5 ± 1.0 °C) except for 16.1 mM where the data for two temperatures were provided. Other conditions as in Fig. 7.
[b] Data for nitrogen formation.

nitrate reduction, other reactions (e.g. N_2 to NH_3) and hydrogen evolution, etc. In dilute nitrate solution, the electrolysis was dominated by molecular hydrogen evolution than by the reduction of nitrate. Also, mass transfer of the reactants to the cathode surface was expected to play an important role in the behaviour of the reactor in such a solution, and consequently, much lower current efficiencies were observed in dilute solutions, compared to the concentrated solutions [43]. Current efficiency also decreased with the electrolysis time in each solution, since nitrate concentration decreased with time, the hydrogen evolution gradually increased to a greater extent and the current efficiency for nitrate reduction decreased. Increase in nitrate concentration significantly reduced energy consumption, e.g. after 24 h electrolysis, 4637.4, 927.0, 34.5 and 37.1 kWh kg^{-1} in 0.1, 1.0, 16.1 and 100 mM nitrate solutions, respectively (Table 2). The much higher energy consumptions in the dilute solutions were a direct consequence of the much lower current efficiencies in these solutions; also, in the dilute nitrate solution, the hydrogen evolution reaction affected the electrode potential and, thus, increased cell voltage to a greater extent than the nitrate reduction [43]. In our case, an increase in nitrate concentration from 0.1 to 100 mM led to a decrease of 0.5 V in cell voltage (Table 3). The selectivity of nitrate reduction was approximately constant over the investigated range of nitrate concentration (Table 3).

The influence of the reaction temperature on nitrate reduction in the ZGSPE reactor was investigated between ambient and 80 °C and typical results are shown in Fig. 7 and Table 3. Increasing temperature favoured ammonia formation and reduced nitrogen formation. One of the reasons was due to different pH change of the catholyte at different temperature during the electrolysis, e.g. at 24 h, the catholyte pH changed from 7.65 to 9.61 and 10.34 at ambient temperature and 80 °C, respectively. The pH change was a natural result of the related reactions (Eqs. (1), (2), (3a), (3b)). In basic nitrate solutions, increasing pH could suppress hydrogen evolution and increase ammonia formation [74]. Consequently, current efficiency for nitrogen formation decreased slightly when the temperature was increased from ambient temperature to 80 °C (Table 3).

The percentage of nitrate removal, space–time yield and rate of nitrate removal increased with increasing temperature, although the effect was relatively small, compared with that of nitrate concentration. For example, the rate of nitrate removal at 80 °C was initially three times higher than that at ambient temperature (Fig. 7) and only increased 0.005 mol cm^{-2} h^{-1} after 24 h, because the nitrate concentration was much higher initially than at 24 h. As the temperature increased, the energy consumption decreased, e.g. at 24 h, 34.5 and 21.0 kWh kg^{-1} at ambient and 80 °C, respectively. This was mainly due to the decrease in the cell voltage, i.e. 2.1 and 1.1 V at ambient and 80 °C, respectively (Table 3).

A relatively small effect of increasing the flow rate from 50 to 100 cm^3 min^{-1} on the rate of nitrate removal was observed, i.e. only changed about 0.003 mol m^{-2} h^{-1} (Fig. 7). This can

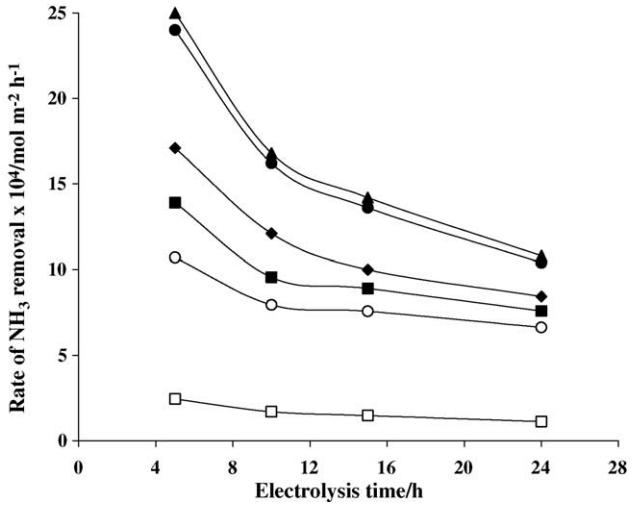

Fig. 8. Effect of temperature and ammonia concentration on rate of ammonia removal during the paired electrolysis in a zero gap solid polymer electrolyte reactor. Temperature and concentration of ammonia (the anolytes were in the simulated solution, 170 cm^3): (■) 22 ± 1.2 °C, 0.38 mM; (□) 22 ± 1.2 °C, 0.06 mM; (◯) 20 ± 1.0 °C, 0.38 mM, 100 cm^3 min^{-1}; (♦) 40 °C, 0.38 mM; (●) 60 °C, 0.38 mM; (▲) 80 °C, 0.38 mM. Other conditions as in Fig. 4.

be attributed to similar conditions in mass transfer and contact time between the catalysts and the reactant at the two flow rates ([6] and the refs. cited in).

Fig. 8 and Table 4 show the effect of ammonia concentration, temperature and flow rate on ammonia oxidation in the ZGSPE reactor using a Pt/Ti mini-mesh anode at a current density of 5 mA cm^{-2} in the simulated solution. In the dilute solutions, e.g. between 0.062 and 0.38 mM, the rate of ammonia removal and the space–time yield were doubled when the concentration was doubled. A significant change occurred when the concentration was increased from 0.38 to 9.42 mM, e.g. at 24 h, values were 0.0011–0.128 mol cm^{-2} h^{-1} and 0.013–9.8 kg m^{-3} h^{-1}. As a result of increased reactant concentration and thus mass transfer. Current efficiency for the nitrogen formation increased from 0.02 to 0.09% when the concentration increased from 0.38 to 9.42 mM (Table 4). Current efficiency also decreased with electrolysis time for each solution, since ammonia concentration decreased with time, the hydrogen evolution gradually increased and current efficiency for nitrogen formation decreased. Another reason for this time dependence was an increased coverage of adsorbed nitrogen adatoms on the electrode, which slowly increased with time and decreased the available area for NH_3 adsorption and dehydrogenation of the adsorbed ammonia to the active intermediates [63]. Improvement in selectivity and inhibition of hydrogen evolution are necessary to increase current efficiency. As a consequence of very low current efficiencies, the energy consumed for the ammonia oxidation was extremely high up to 5070 kWh kg^{-1} (Table 4), although we can essentially ignore these high values because of the nature of the paired electrolysis.

Table 4
Effect of concentration of ammonia and temperature on the paired electrolysis—ammonia oxidation[a]

	Concentration (mM)				
	0.062	0.17	0.38	0.38 (80 °C)	9.42
χ (%)	100	100	82.4	100	35.7
γ (kg m^{-3} h^{-1})	0.002	0.006	0.013	0.015	9.8
β (mol cm^{-2} h^{-1})	0.0004	0.0006	0.0011	0.0014	0.128
ξ_{NO_2} (%)	0	0	0	0	0
ξ_{NH_3} (%)	34.8	42.2	47.0	62.0	45.2
ξ_{N_2} (%)	65.2	57.8	53.0	38.0	54.8
ϕ (%)[b]	0.02	0.05	0.078	0.08	0.09
ψ (kWh kg^{-1})	5070.4	1965.0	261.0	403.8	590.2
E_{cell} (V)	2.2	2.1	2.1	1.1	2.0

[a] Data were collected at 24 h and ambient temperature (21.5 ± 1.0 °C) except for 0.38 mM where the data for two temperatures were provided. Other conditions as in Fig. 8.
[b] Data for nitrogen formation.

There were small changes in the cell voltage with changing concentrations of nitrate and ammonia (Tables 3 and 4), suggesting that a relatively small concentration polarisation due to the high ion concentrations of the simulated solution. The cell voltage decreased significantly with increasing temperature, e.g. from 2.1 to 1.1 V for an increase in the temperature from ambient to 80 °C, which were direct results of enhanced reaction kinetics on the anode and cathode and increase in the electrolyte conductivities.

Increasing temperature from ambient to 80 °C increased the percentage and rate of ammonia removal and the space–time yield from 82.4 to 100%, 0.013 to 0.015 kg m^{-3} h^{-1} and 0.0011 to 0.0014 mol cm^{-2} h^{-1} at 24 h (Fig. 8 and Table 4), respectively, due to the enhanced reaction kinetics. More nitrate ions were produced and less nitrogen was evolved at elevated temperature, compared to low temperature during ammonia oxidation (Table 4).

Increasing the flow rate above 50 cm^3 min^{-1}, e.g. to 100 cm^3 min^{-1}, led to a decrease in the rate of ammonia removal (Fig. 8), suggesting that the contact time between the catalysts and the reactant had greater impact on the oxidation rate than mass transfer.

3.5. Bulk electrolysis—influence of electrolysis media

Table 5 compares the paired electrolysis in the ZGSPE reactor with alkaline solution or with pure water. Similar results were obtained in the two media, although the oxidation of ammonia in pure water seemed slightly better than in the alkaline solution. The implication of such data is that the technology will potentially attract wide applications including wastewaters with very low levels of nitrate and ammonia.

The main problems with electrolysis were production of nitrate and nitrite ions during the oxidation of ammonia, especially for long-term operation. A change in the operating conditions, e.g. decreasing current density, could partially suppress this trend, although more efficient approaches, e.g. selective anode materials, are required to tackle the problems thoroughly.

Table 5
Effect of medium on the paired electrolysis in a ZGSPE reactor[a]

Medium	$NaHCO_3$ (NO_3^-)	H_2O (NO_3^-)[b]	$NaHCO_3$ (NH_3)	H_2O (NH_3)[b]
χ (%)	56.8	54.6	99.2	99.4
γ (kg m^{-3} h^{-1})	8.3	8.4	0.14	0.15
β (mol cm^{-2} h^{-1})	0.11	0.10	0.022	0.019
ξ_{NO_2} (%)	0	0	16.7	11.1
ξ_{NH_3} (%)	12.7	10.4		
ξ_{NO_3} (%)			23.8	22.4
ξ_{N_2} (%)	87.3	89.6	59.5	65.5
ϕ (%)[c]	24.6	24.3	3.0	3.8
ψ (kWh kg^{-1})	43.2	46.1	65.6	55.6
E_{cell} (V)	2.9	2.8	2.9	2.6

[a] All parameters were collected at 45 h. The conditions as in Fig. 4.
[b] Pure water solution with the same concentrations of nitrate and ammonium as in Fig. 4.
[c] Data for nitrogen formation.

3.6. Comparison between single and paired electrolysis

The most important advantage of the paired electrolysis is the full use of both cathode and anode for the useful electrochemical conversion rather than only allowed a side reaction in one side. The paired electrolysis sorted out problems caused by the unavoidable production of ammonia during treatment of nitrate. So the waste stream could be put into a closed loop to realise the total elimination of nitrate as well as ammonia, if any. Selectivity for the both cathode and anode should be improved in order to increase competitiveness of the technology, compared with the current routine methods.

Our data are similar or better than some reported results, e.g. reduction of the nitrate concentration from 600 to 50 mg dm^{-3} with a current efficiency of 22% and ammonia as a main product, during the nitrate reduction in $NaHCO_3$ solutions at a copper plate cathode in an undivided flow-through reactor [17]. Compared to our data, higher current efficiency, e.g. 40%, and very low energy consumption, e.g. 0.05 kWh kg^{-1}, have been reported for the ammonia oxidation [2,10,44]. These data indicate new research directions, e.g. use of three-dimensional materials in ZGSPE reactors to enhance mass transfer and increase process efficiency.

4. Conclusions

Simultaneous reduction of nitrate and oxidation of ammonia is feasible in a zero gap solid polymer reactor, which made it possible to treat generated ammonia during nitrate reduction. Complete removal of 16.1 mM nitrate and 9.4 mM ammonia was achieved within 45 h with removal rates of 0.057 mol NO_3 cm^{-2} h^{-1} and 0.017 mol NH_3 cm^{-2} h^{-1} and current efficiencies for nitrogen formation of 24.5% in the nitrate reduction and 1.4% in the ammonia oxidation. The selectivity was promising for the nitrate reduction, i.e. no nitrite was formed and N_2 was the main product under the best conditions but an improvement is required to increase selectivity for the ammonia oxidation towards nitrogen. A major benefit for the paired electrolysis is the energy savings resulting from the simultaneous use of cathode and anode reactions.

The rates of nitrate and ammonia removal, the space–time yield and the current efficiency increased significantly and the energy consumption decreased significantly with increasing nitrate concentration. Percentages of nitrate and ammonia removal, space–time yield and rate of nitrate removal increased with increasing temperature. Increasing temperature favoured the side reactions, e.g. formation of ammonia in nitrate reduction and production of nitrate and nitrite in ammonia oxidation.

The paired electrolysis in the ZGSPE reactor could be carried out in pure water without additional supporting electrolytes, which demonstrated the technology is applicable to a wide range of wastewater including those with very low levels of nitrate and ammonia.

Further work is necessary to find and optimise selective materials for reduction of nitrate and oxidation of ammonia toward to nitrogen, in order to achieve higher competitiveness. Use of an anion exchange membrane is another aspect to fully explore the advantages of the ZGSPE reactor for the paired electrolysis.

Acknowledgements

The authors thank the United Kingdom Engineering and Physical Sciences Research Council (EPSRC) for funding. The work was performed in research facilities provided through an EPSRC/HEFCE Joint Infrastructure Fund award (No. JIF4NESCEQ).

References

[1] N.F. Gray, Drinking Water Quality: Problems and Solutions, John Wiley and Sons Ltd., Chichester, 1994, p. 21.
[2] J.O'M. Bockris, J. Kim, J. Appl. Electrochem. 27 (1997) 623.
[3] http://www.cmst.org/OTD/tech_summs/ESPIP/ESPIP_chap4.4.html.
[4] A.C.A. de Vooys, M.T.M. Koper, R.A. van Santen, J.A.R. van Veen, JEC 506 (2001) 127.
[5] M. Badea, A. Amine, G. Palleschi, D. Moscone, G. Volpe, A. Curulli, J. Electroanal. Chem. 509 (2001) 66.
[6] K. Lüdtke, K.-V. Peinemann, V. Kasche, R.-D. Behling, J. Membr. Sci. 151 (1998) 3.
[7] http://www.ohd.hr.state.or.us/dwp/docs/fact/ammonia.pdf.
[8] EEC Council Recommendations, 1987.
[9] EEC Council Directive 98/83/EC.
[10] M. Paidar, K. Bouzek, H. Bergman, Chem. Eng. J. 85 (2002) 99.
[11] http://www.lanl.gov/projects/nitrate/Other.htm.
[12] http://www.cmst.org/OTD/tech_summs/MWIP/MWIP_chap3.1.3.html.
[13] K. Bouzek, M. Paidar, A. Sadilkova, H. Bergmann, J. Appl. Electrochem. 31 (2001) 1185.
[14] C.-P. Huang, H.-W. Wang, P.-C. Chiu, Wat. Res. 32 (1998) 2257.
[15] A. Kapoor, T. Viraraghavan, J. Environ. Eng. 123 (1997) 371.
[16] V. Tripathi, Chemical Engineering, M.Sc. Thesis, Montana State University, April, 1997.
[17] M. Paidar, I. Rousar, K. Bouzek, J. Appl. Electrochem. 29 (1999) 611.

[18] O.M. Ilinitch, L.V. Nosova, V.V. Gorodetskii, V.P. Ivanov, S.N. Trukhan, E.N. Gribov, S.V. Bogdanov, F.P. Cuperus, J. Mol. Catal. A Chem. 158 (2000) 237.
[19] S.R. Gavagnin, F. Pinna, E. Modaferri, S. Perathoner, G. Centi, M. Marella, M. Tomaselli, Catal. Today 55 (2002) 139.
[20] K.M. Hiscock, J.W. Lloyd, D.N. Lemer, Wat. Res. 25 (1991) 1099.
[21] C.L. Clement, N.A. Nado, A. Katty, M. Bernard, A. Deneuville, C. Comninellis, A. Fujishima, Diamond Relat. Mater. 12 (2003) 606.
[22] J.O'M. Bockris, J. Kim, J. Electrochem. Soc. 143 (1996) 3801.
[23] J. Kaczur, D. Cawlfield, K. Woodart Jr., US Patent Appl. 5,376,240 (1994).
[24] J.D. Genders, D. Hartsough, D.I. Hobbs, J. Appl. Electrochem. 26 (1996) 1.
[25] E.E. Kalu, R.E. White, D.I. Hobbs, J. Electrochem. Soc. 143 (1996) 3094.
[26] D.R. Lide, H.P.R. Frederikse (Eds.), CRC Handbook of Chemistry and Physics, Section 8, 78th ed., CRC Press, New York, 1997.
[27] W.J. Plieth, in: A.J. Bard (Ed.), Encyclopaedia of Electrochemistry of the Elements, vol. VIII, Marcel Dekker, 1978 (Chapter 5).
[28] H.G. Oswin, M. Salomon, Can. J. Chem. 41 (1963) 1686.
[29] L. Marincic, F.B. Leitz, J. Appl. Electrochem. 8 (1978) 333.
[30] A.R. Despic, D.M. Drazic, P.M. Rakin, Electrochim. Acta 11 (1966) 997.
[31] G.E. Dima, A.C.A. de Vooys, M.T.M. Koper, J. Electroanal. Chem. 554–555 (2003) 15.
[32] M.T. de Groot, M.T.M. Koper, J. Electroanal. Chem. 562 (2004) 81.
[33] H.-L. Li, J.Q. Chambers, J. Appl. Electrochem. 18 (1988) 454.
[34] J.F.E. Gootzen, L. Lefferts, J.A.R. van Veen, Appl. Catal. A Gen. 188 (1999) 127.
[35] J.F.E. Gootzen, P.G.J.M. Peeters, J.M.B. Dukers, L. Lefferts, W. Visscher, J.A.R. van Veen, J. Electroanal. Chem. 434 (1997) 171.
[36] A.C.A. de Vooys, R.A. van Santen, J.A.R. van Veen, J. Mol. Catal. A Chem. 154 (2000) 203.
[37] IONEX Ltd., British Patent Appl. 2,348,209 (2001).
[38] F. Bouamrane, A. Tadjeddine, J.E. Butler, J. Electroanal. Chem. 405 (1996) 95.
[39] C. Reuben, E. Galun, H. Cohen, J. Electroanal. Chem. 396 (1995) 2333.
[40] B. Keita, E. Abdeljalil, L. Nadjo, R. Contant, R. Belgiche, Electrochem. Commun. 3 (2001) 56–62.
[41] W. Sun, S. Zhang, X. Lin, L. Jin, S. Jin, J. Deng, J. Kong, J. Electroanal. Chem. 469 (1999) 63.
[42] N. Chebotareva, T. Nyokong, J. Appl. Electrochem. 27 (1997) 975.
[43] C. Lu, S. Lu, W. Qiu, Q. Liu, Electrochim. Acta 44 (1999) 2193.
[44] A.S. Koparal, U.B. Ogutveren, J. Hazard. Mater. 89 (2002) 83.
[45] S.U. Zarnatu, C. Yanez, Electrochim. Acta 42 (1997) 1725.
[46] N.G. Carpenter, D. Pletcher, Anal. Chim. Acta 317 (1995) 287.
[47] G. Horanyi, E.M. Rizmayer, J. Electroanal. Chem. 140 (1982) 347.
[48] G. Horanyi, E.M. Rizmayer, J. Electroanal. Chem. 143 (1983) 323.
[49] B.R. Scharifker, J. Mostany, A. Serruya, Electrochem. Commun. 2 (2000) 448.
[50] S.-H. Cheng, Y.O. Su, Inorg. Chem. 33 (1994) 5847.
[51] A.B.P. Lever, M.R. Hempstead, C.C. Leznoff, W. Liu, M. Melnik, W.A. Nevin, P. Seymour, Pure Appl. Chem. 58 (1986) 1467.
[52] G. Horanyi, R.M. Ritzmayer, JES 188 (1985) 273.
[53] D. Pletcher, Z. Poorabedi, Electrochim. Acta 24 (1979) 1253.
[54] S. Cattarin, J. Appl. Electrochem. 22 (1992) 1077.
[55] D. Dutta, D. Landolt, Electrochim. Acta 119 (1972) 1320.
[56] L.J. Sealock Jr., D.C. Elliott, E.G. Baker, A.G. Fassbender, L.J. Silva, Ind. Eng. Chem. Res. 35 (1996) 4111.
[57] T. Katan, R.G. Galiotto, J. Electrochem. Soc. 110 (1963) 1022.
[58] D.-M. Pfennig, J. Deprez, D. Kitzelmann, Ber. Bunsenges. Phys. Chem. 94 (1990) 988.
[59] A.R. Despic, D.M. Drazic, P.M. Rakin, Electrochim. Acta 11 (1966) 997.
[60] K. Sasaki, Y. Hisatomi, J. Electrochem. Soc. 117 (1970) 758.
[61] L. Marincic, F.B. Leitz, J. Appl. Electrochem. 8 (1978) 333.
[62] A.C.A. de Vooys, M.T.M. Koper, R.T. van Santen, J.A.R. van Veen, J. Electroanal. Chem. 506 (2001) 127.
[63] J.F.E. Gootzen, A.H. Wonders, W. Visscher, R.A. van Santen, J.A.R. van Veen, Electrochim. Acta 43 (1998) 1851.
[64] H. Gerischer, A. Maurerer, J. Electroanal. Chem. 25 (1970) 421.
[65] B.A. Lopez de Mishima, D. lescano, T.M. Holgado, H.T. Mishima, Electrochim. Acta 43 (1998) 395.
[66] R. Ukropec, B.F.M. Kuster, J.C. Schouten, R.A. van Santen, Appl. Catal. B 23 (1999) 45.
[67] H. Cheng, K. Scott, P.A. Christensen, J. Appl. Electrochem. 33 (2003) 893.
[68] H. Cheng, K. Scott, J. Power Sources 123 (2003) 137.
[69] A.I. Vogel, revised by G.H. Joffery, J. Bassett, J. Mendham, R.C. Denney, Vogel's Textbook of Quantitative Chemical Analysis, fifth ed., Longman Scientific & Technical, p. 408 or pp. 402–403 for determination of hydroxylamine or hadrazine, respectively.
[70] F. Goodridge, K. Scott, Electrochemical Process Engineering, Plenum Press, New York, 1995, pp. 15–191.
[71] D. Pletcher, F.C. Walsh, Industrial Electrochemistry, second ed., Chapman and Hall, New York, 1990 (Chapter 2).
[72] C.P. De Pauli, S. Trasatti, J. Electroanal. Chem. 396 (1995) 161.
[73] C.L.P.S. Zanta, A.R. de Andrade, J.F.C. Boodts, Electrochim. Acta 44 (1999) 3333.
[74] T. Ohmori, M.S. El-Deab, M. Osawa, J. Electroanal. Chem. 470 (1999) 46.
[75] R. Tenne, C.C. Clement, Isr. J. Chem. 38 (1998) 57.
[76] D.W. McKee, A.J. Scarpellino Jr., I.F. Danzig, M.S. Pak, J. Electrochem. Soc. 116 (1969) 562.
[77] N. Alonso-Vante, in: A. Wieskowki, E.R. Sauliroua, C. Vayeras (Eds.), Catalysis and Electrocatalysis at Nonoparticle Surfaces, Marcel Dekker, New York, 2003.
[78] L. Guczi, J. Mol. Catal. 25 (1984) 13.
[79] S. Wasmus, E.J. Vasini, M. Krausa, H.T. Mishima, W. Vielstich, Electrochim. Acta 39 (1994) 23.
[80] A.C.A. de Vooys, M.T.M. Koper, R.A. van Santen, J.A.R. van Veen, Electrochim. Acta 46 (2001) 923.
[81] K. Hara, M. Kamata, N. Sonoyama, T. Sakata, J. Electroanal. Chem. 451 (1998) 181.